Electronic Supplementary Material (ESI) for ChemComm.

Limiting sulfur and mastering the diffusion of lithium ions with cerium oxide-based porous carbon rods

Yuhang Shan[a], Libo Li[a]*

Section 1 Experimental Section

Ⅰ. Material and General Methods

All chemicals such as Soy protein isolate, Sodium citrate, and Cerium nitrate were analytical grades and directly used without any purification. The phase composition of CeO_2/PCR, PCR, and CR materials was tested by Cu Kα radiation with X 'Pertpro X-ray Diffraction (XRD) with the 2θ range from 10° to 90°) at room temperature. The scanning electron microscope (SEM, FEI-Sirion200) characterized the morphology of CR, PCR, and CeO_2/PCR materials. A transmission electron microscope (TEM, JEM-2100) further observed their structures. The X-ray photoelectron spectroscopy (XPS, PHI5700, American physical electronics) determined the chemical state of C, Ce and S elements.

The cathode was cut into a circular plate with a diameter of 14 mm. The assembly of LIR2025 coin batteries was carried out in a glove box under the protection of argon. The land-CT2001A battery measured the galvanostatic charge-discharge performance of the lithium-sulfur battery with a voltage range from 1.7 V to 2.8 V at room temperature. CHI760E electrochemical workstation tested Cyclic voltammetry curves (CV) with the voltage scanning range of 1.5~3 V, and the scanning speed was 0.1 mV s^{-1}. Celgard 2500

membrane was used as the separator and the electrolyte consisted of 1 mol L^{-1} lithium bis(trifluoromethanesulfonic) imide (LiTFSI) in a mixture of 1, 3-dioxolane (DOL) and dimethoxymethane (DME) (1:1, v/v) with 1 wt.% $LiNO_3$. The anode was lithium foil of 15.6 mm diameter and 1 mm thickness. Electrochemical impedance spectroscopy (EIS) was performed on the CHI760E electrochemical station with 0.01 Hz~10^5 Hz at room temperature. Tafel slope was tested on CHI760E with a voltage range from 2.4 V to 2.0 V, and the scanning rate was 5 mV s^{-1}.

Nucleation measurements

0.4 mol L^{-1} Li_2S_8 solution was prepared by violently stirring lithium sulfide (Li_2S) and sulfur powder in tetraethylene glycol dimethyl ether at the molar ratio of 1:7. CR, PCR, and CeO_2/PCR were used as nucleation substrates to assemble the cell, and lithium foil was used as the anode. During the battery assembly, 25 μL of Li_2S_8 (0.4 mol L^{-1}) was dropped onto the cathode, and then 25 μL of electrolytic liquid without Li_2S_8 was dropped on the lithium anode side. The battery was performed galvanostatic discharge to 2.06 V under the current of 0.112 mA, and the potential was then kept at 2.05 V until the current dropped below 10^{-5} mA.

CV of Li_2S_6 symmetric cells

0.2 mol L^{-1} Li_2S_6 solution was prepared by violently stirring lithium sulfide (Li_2S) and sulfur powder in 1:1 (v/v) DOL/DME at the molar ratio of 1:5. CR, PCR and CeO_2/PCR were used as working electrode and counter electrode. And

40 μL electrolyte of 0.1 M Li_2S_6 in a 1:1 (v/v) DOL/DME mixture was added to both sides of the PP separator. CV was measured at a scanning rate of 10 mV s^{-1} between -0.7 V and 0.7 V for symmetric batteries.

The calculations were based on Density Functional Theory (DFT), as implemented in the CASTEP module. The exchange-correlation functional selected the generalized gradient approximation of the Perdew-Burke-Ernzerhof (GGA-PBE) functional. Eq. (3) is the energy calculation formula.

$$E_{\text{Binding Energy}} = E_{\text{Total}} - (E_1 + E_2)$$

Ⅱ. Synthesis of CR, PCR and CeO_2/PCR materials.

2 g soy protein isolate (SPI) and 0.7g sodium citrate were dispersed in deionized water. Adjust pH to 9 until the SPI was completely dissolved. The solution was heated to 60 ^{0}C and aged to a gel state. It was transferred to a tubular furnace and heated to 850 ^{0}C under nitrogen for 3 h. The CR material was obtained after cooling. The CR material and KOH were dispersed in deionized water according to the mass ratio of 1:2, and the ultrasonic treatment lasted for 1 h. Dry the water in a vacuum oven at 100 ^{0}C. The mixture was transferred to a tubular furnace and heated to 800 ^{0}C under nitrogen for 2 h to obtain a black powder. The black powder was dispersed in deionized water and an excess of 10% HCl solution was added until no bubbles formed. The PCR materials were centrifuged with ethanol and dried. The PCR materials, ammonium acetate, urea, and cerium nitrate were

dispersed in ethanol in a certain proportion, then transferred to a high-pressure kettle and heated at 120 ^{0}C for 24 h. CeO_2/PCR materials were obtained by repeated centrifugation with ethanol/deionized water after drying. CR, PCR, and CeO_2/PCR materials material was mixed with sulfur according to the mass ratio of 1:4, and heated to 155 ^{0}C in N_2 atmosphere for 6 h to obtain S@CR, S@PCR, and S@CeO_2/PCR materials.

Section 2 Supplementary structural figures and characterization information

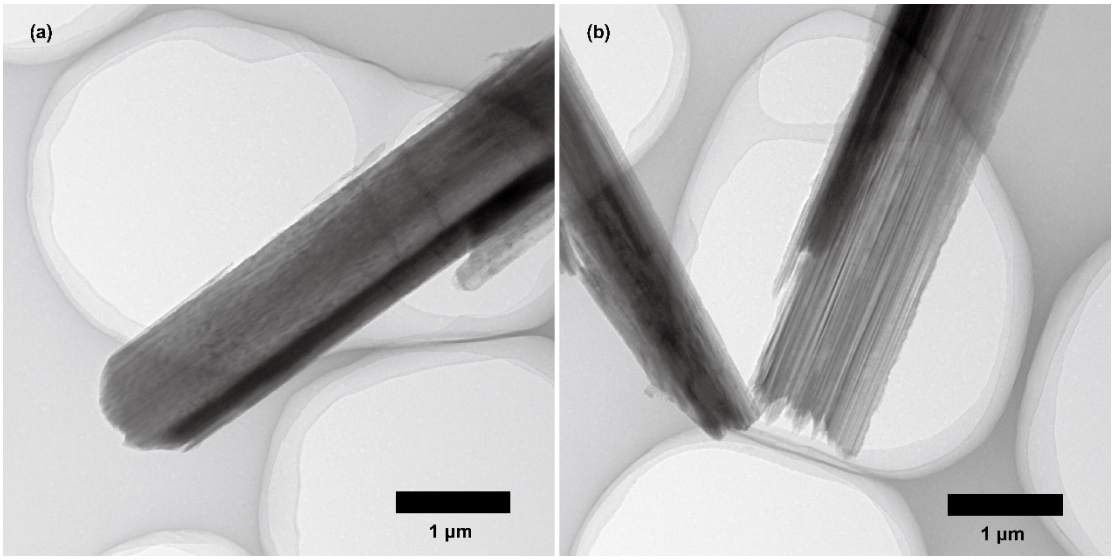

Figure S1. TEM image of CR material.

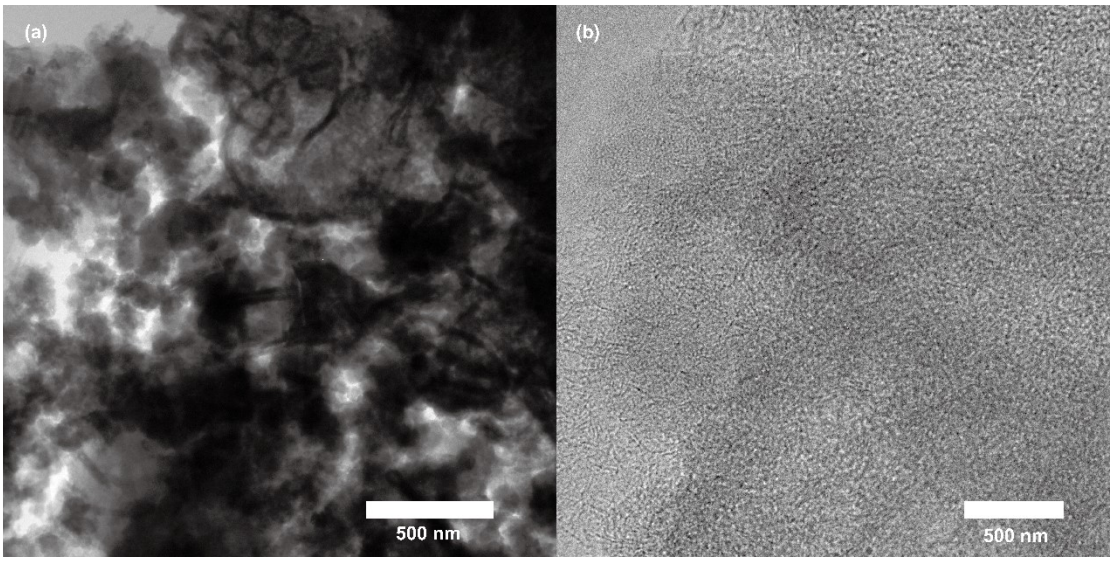

Figure S2. TEM image of PCR material.

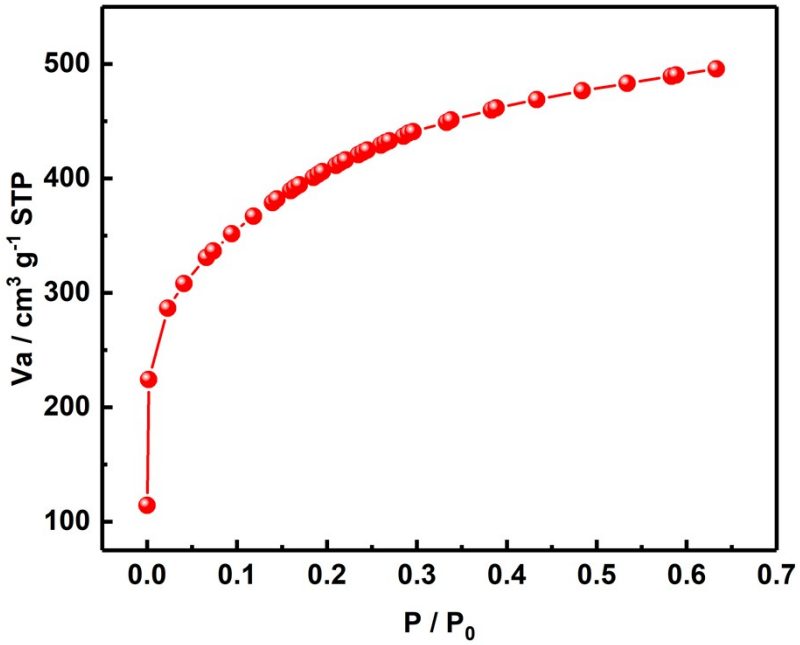

Figure S3. Adsorption isotherms of PCR materials.

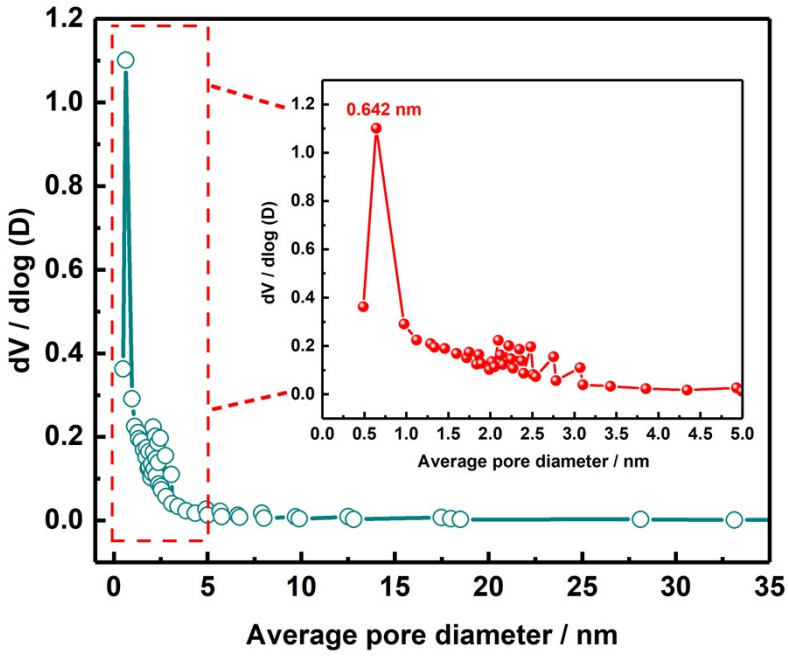

Figure S4. Pore size distribution curves of PCR materials.

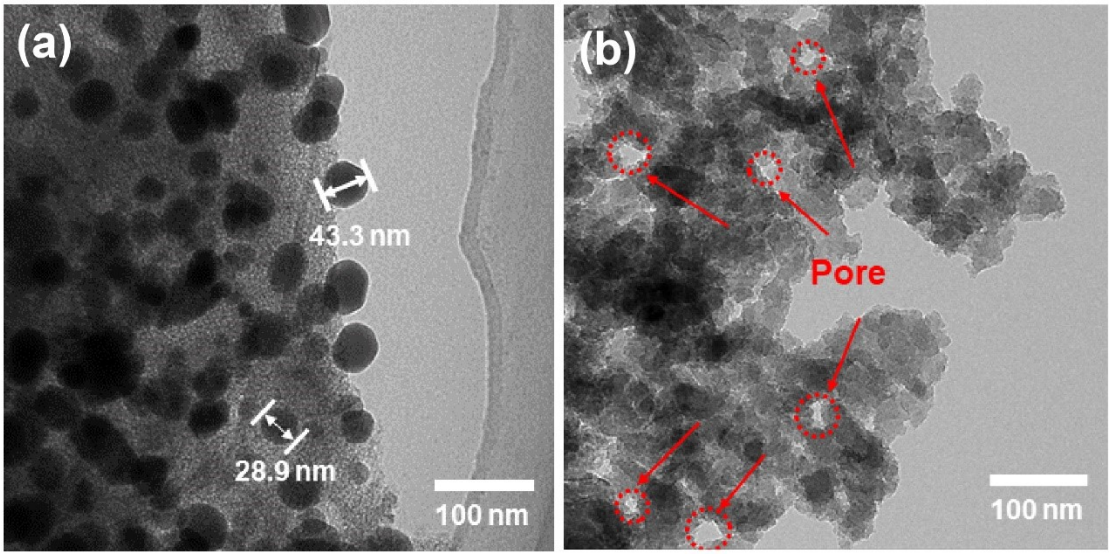

Figure S5. Comparison of PCR materials before and after embedding CeO_2 with the same scale.

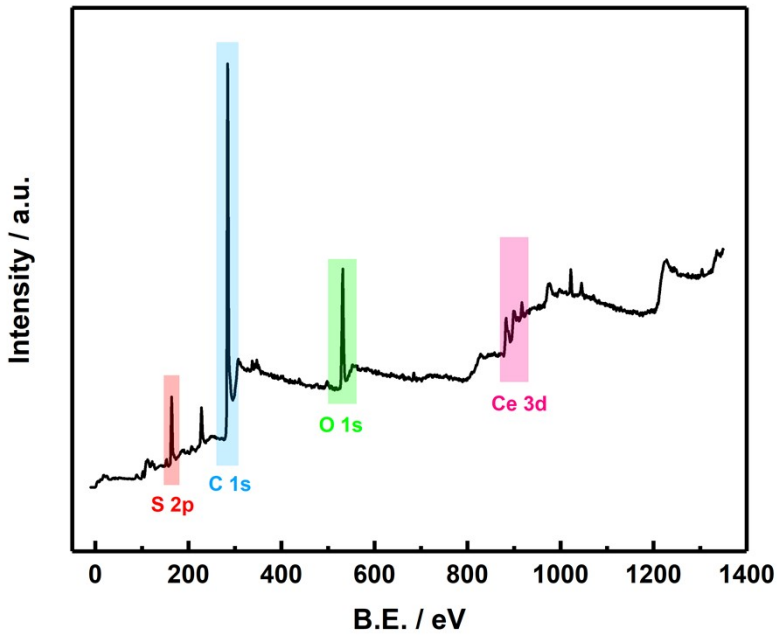

Figure S6. Full spectrum of XPS analysis

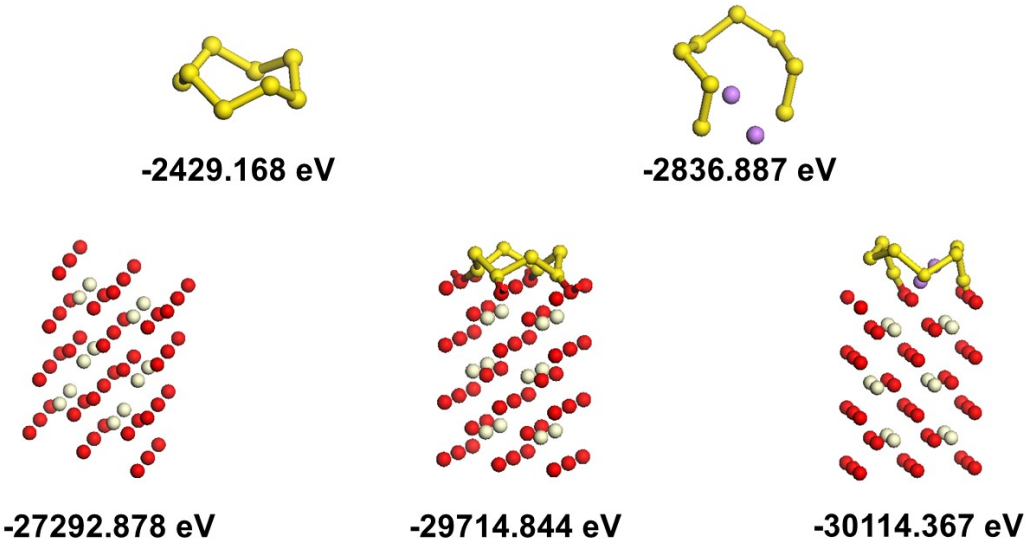

Figure S7. The optimized structures and the energy of CeO_2, S_8 and Li_2S_8.

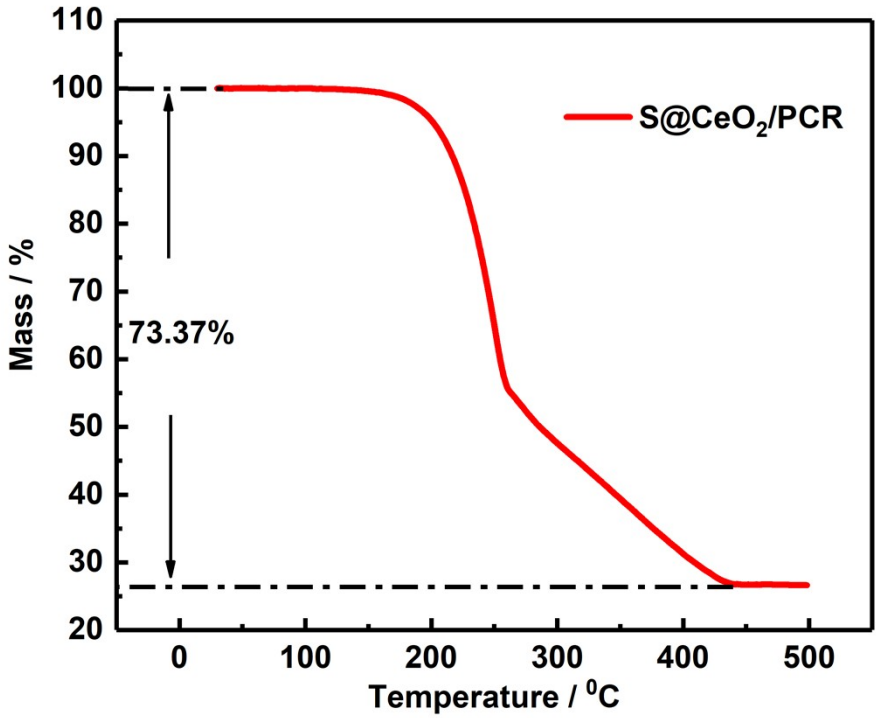

Figure S8. TG test of $S@CeO_2/PCR$.

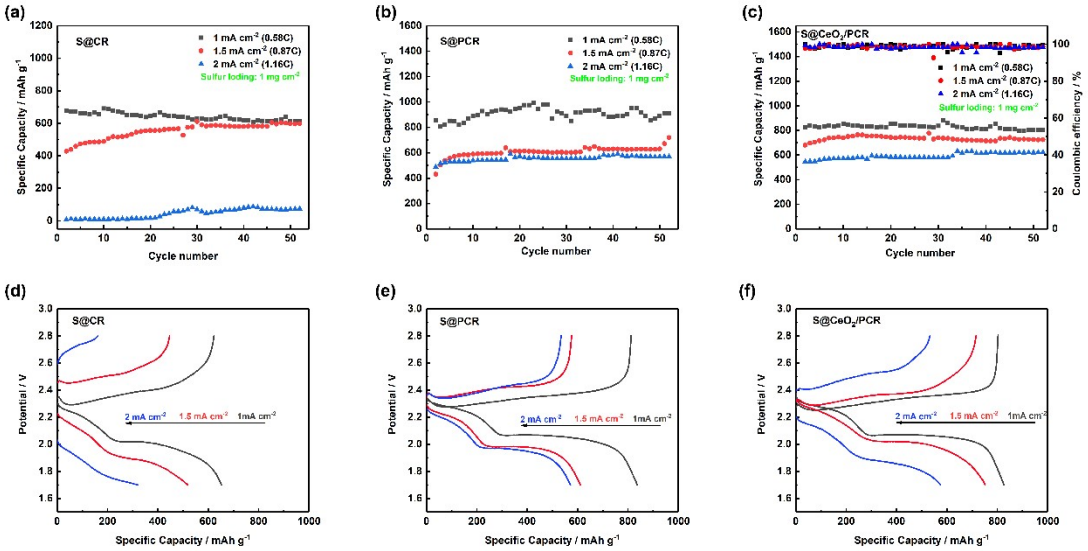

Figure S9. Polarization voltage curves at different current densities.

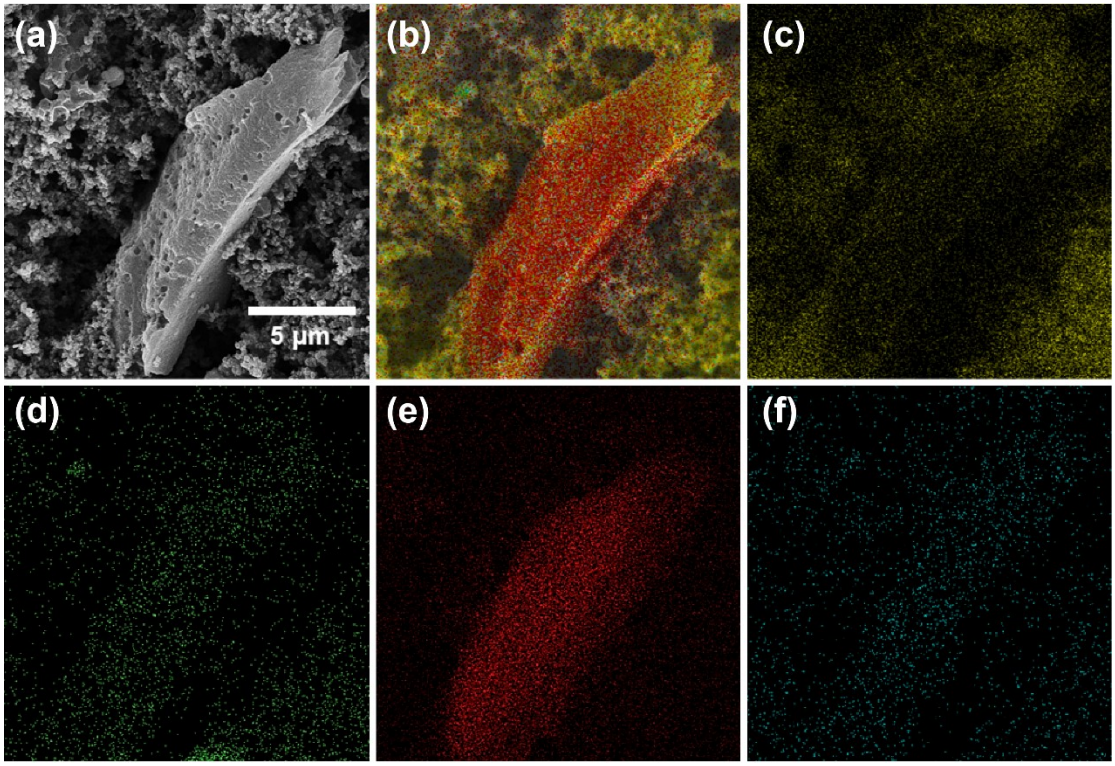

Figure S10. SEM of CeO_2/PCR cathode after 100 cycles.

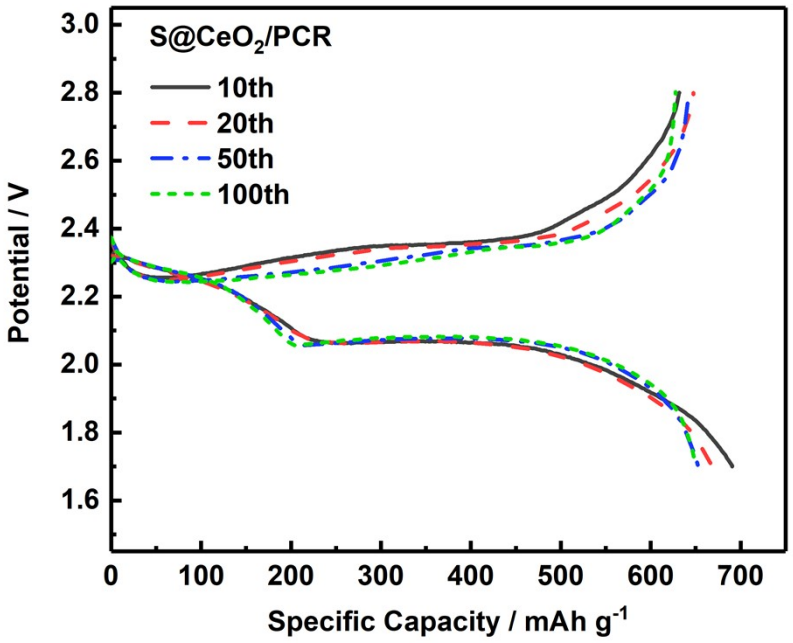

Figure S11. Specific capacity-voltage curve of S@CeO_2/PCR.

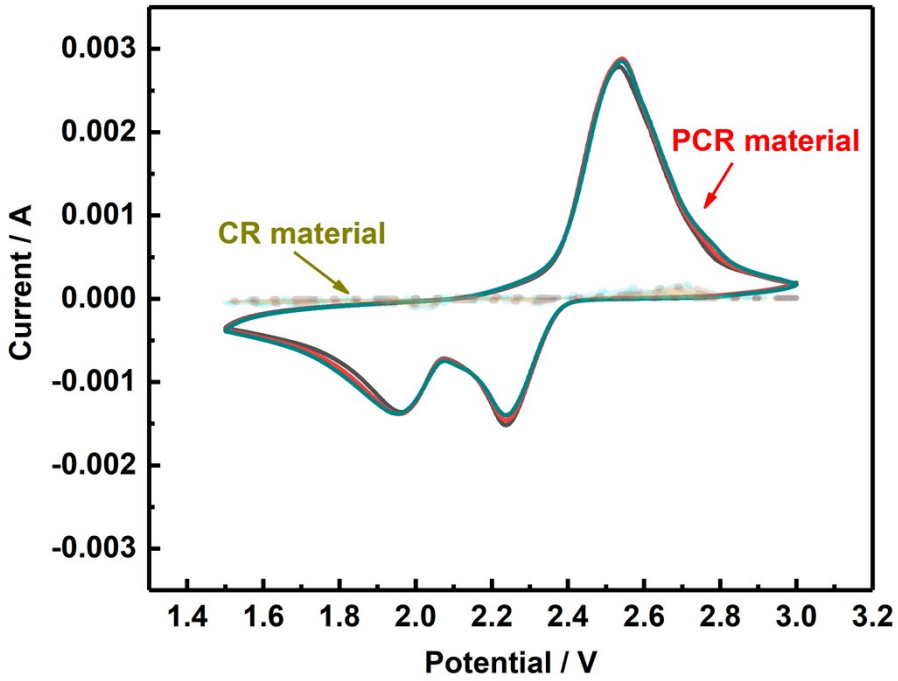

Figure S12. CV curves of S@PCR and S@CR.

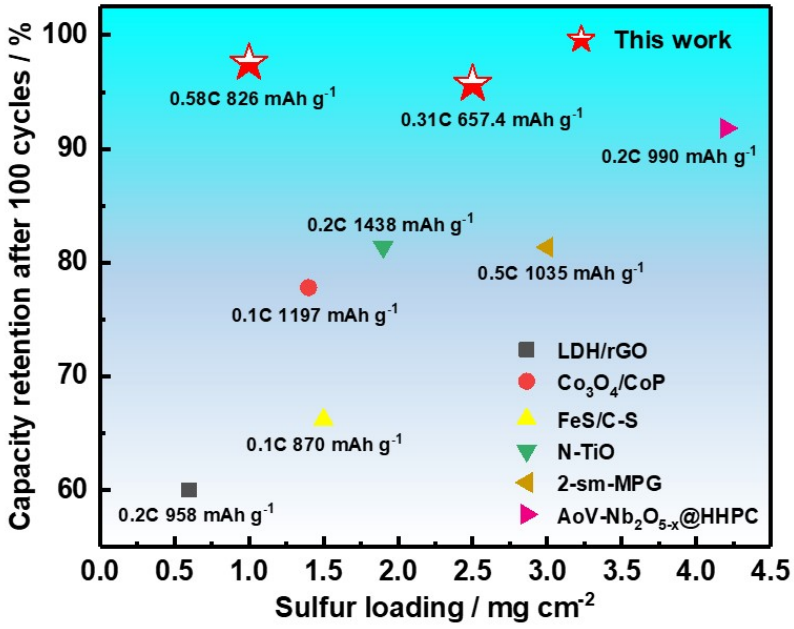

Figure S13. Comparison of the sulfur loading and capacity retention of CeO_2/PCR with previously reports.

Table S1 Comparison of specific capacity and capacity retention with previously reports.

Materials	Sulfur loading	C-rate	Initial specific capacity / Capacity retention	Reference
LDH/rGO	0.6 mg cm^{-2}	0.2C	958 mAh g^{-1}/ 60%	1
Co_3O_4/CoP	1.4 mg cm^{-2}	0.1C	1197 mAh g^{-1} / 77.8%	2
FeS/C-S	1.5 mg cm^{-2}	0.1C	870 mAh g^{-1}/ 66.2%	3
N-TiO	1.9 mg cm^{-2}	0.2C	1438 mAh g^{-1}/ 81.36%	4
2-sm-MPG	3 mg cm^{-2}	0.5C	1035 mAh g^{-1} / 81.35%	5
AoV-Nb_2O_{5-x}@HHPC	4.2 mg cm^{-2}	0.2C	1197 mAh g^{-1}/ 77.8%	6
This work	**1 mg cm^{-2}**	**0.58C**	**826.2 mAh g^{-1}/ 97.57%**	**-**
This work	**2.5 mg cm^{-2}**	**0.31C**	**657.4 mAh g^{-1}/ 95.71%**	**-**

Notes and references

1 F. Xu, C. Dong, B. Jin, H. Li, Z. Wen, Q. Jiang, Electroanal. Chem, 2020, **876**, 114545.

2 D. Wang, D. Luo, Y. Zhang, Y. Zhao, G. Zhou, L. Shui, Z. Chen, X. Wang, Nano Energy, 2021, **81**, 105602.

3 Q. Yuan, Y. Chen, A. Li, Y. Li, X. Chen, M. Jia, H. Song, Appl. Surf. Sci. 2020, **508**, 145286.

4 M. Li, Y. Zhu, X. Wu, Y. Lei, X. He, Q. Li, R. Jiang, Z. Lei, Z. Liu, and J. Sun, ACS App. Energy Mater. 2021, **4**, 5713-5736.

5 B. Liu, S. Gu, H. Li, Y. Wang, Y. He, X. Song, G. Zhou, Mater. Today Energy, 2020, **17**, 100484.

6 S. Cheng, J. Wang, S. Duan, J. Zhang, Q. Wang, Y. Zhang, L. Li, H. Liu, Q. Xiao, H. Lin, Chem. Eng. J. 2021, 417, 128172.